Eleventh South African Conference on Computational and Applied Mechanics
SACAM 2018
Vanderbijlpark, South Africa, 17-19 September 2018

On the uniqueness of material identification for aluminium using spherical indentation

Nick Kossolapov[a], Schalk Kok[a]

[a]*Department of Mechanical and Aeronautical Engineer, University of Pretoria, Pretoria, 0028, South Africa*

nickkossolapov@gmail.com, schalk.kok@up.ac.za

Abstract

Indentation tests are often used in material identification where direct measurement methods cannot be used, that is for thin films or because the equipment of interest is in use. However, uniqueness of the identified material parameters is often neglected in the analysis. A virtual indentation test was performed to simulate the force versus deflection curve of the reaction load on the indenter during the indentation, where the true material parameters of a three parameter Voce material model are known beforehand. Using a radial basis function surrogate model, it was shown that not only it is possible for different parameters to produce the same force-deflection curve, but for continuous ranges or families of parameters to produce the same force-deflection curve for significant ranges of the parameters. This shows that there is a one-to-many correspondence between the force-deflection curve and the material parameters. Identified material parameters are often reported without much regard to the uniqueness of the problem. However, the results of the investigation show that the uniqueness of the problem should be placed under more scrutiny for practical applications.

Keywords: Spherical indentation; Strain hardening; Yield strength; Stress–strain curve; Inverse Analysis

1. Introduction

It is often necessary to be able to determine the mechanical properties of the material that certain equipment is manufactured from. If the equipment is in use, non-destructive methods have to be used. A widely used method is performing a micro-indentation test to obtain the applied force versus displacement curve of the indenter on the material, the F-h curve. The yield stress-plastic strain curve can then be extracted from this data through inverse analysis [1].

A numerical study was done to attempt to find the parameter values of a yield stress-plastic strain model using a known F-h curve and finite element analysis. The yield stress model used was a saturation-based relationship, given by Voce [2] as

$$\sigma_y(\varepsilon_p) = \frac{\sigma_0}{1-b}(1 - be^{-m\varepsilon_p}). \tag{1}$$

Here σ_y is the yield stress and ε_p is the equivalent plastic strain. The model has three adjustable material parameters, σ_0, b and m. The numerical analysis was an inverse analysis where the material parameters are adjusted by some optimization routine until the simulated F-h curve matches the known F-h curve. An often neglected aspect of inverse analysis is the uniqueness of the problem. If the inverse problem is sufficiently insensitive to the adjustable parameters many solutions may be found that solve the problem within error.

An investigation on the uniqueness of the inverse problem of material identification when using an indentation test was often not found in literature, particularly with spherical indentation. This paper seeks to empirically investigate the uniqueness, and show that the uniqueness of the problem should not be assumed.

2. Finite Element Simulation of Indentation

The finite element simulation was composed of an axisymmetric model using a spherical indenter. The simulation used bConverge's *CalculiX for Windows* 2.10 running on an Intel i5-7600k. The mesh used is shown in Fig. 1 (a), and was generated using GraphiX, CalculiX's built-in meshing suite. A detail view of the indenter is shown in Fig. 1 (b).

The finite element model was composed of 4-noded axisymmetric elements. Friction was not used in the model to simplify both the simulation and the analysis. The bottom of the material was constrained vertically. The displacement of the top of the indenter was prescribed, and the resulting reaction force was computed.

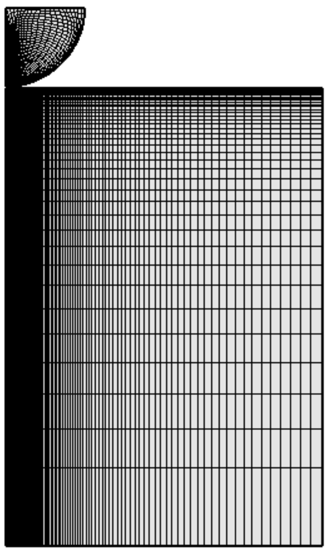

Fig. 1 (a) Axisymmetric model of indentation

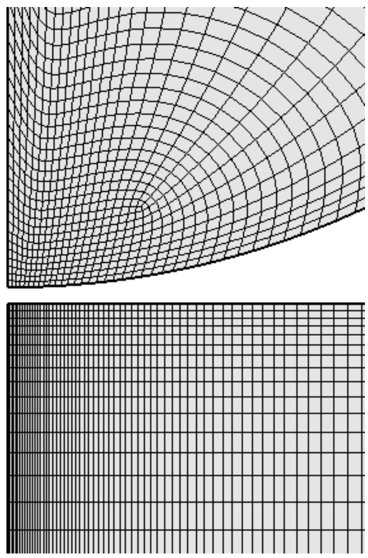

Fig. 1 (b) Detail view of indenter

The indenter was modelled as an elastic body. If the indenter were to experience plastic deformation it would increase the complexity of the problem by introducing an additional stress-strain curve which may not be known a priori. Using a rigid body is often employed for conical indenters [3, 4]. However, this simplification may also be applied to spherical indenters as a brief investigation showed that modelling the indenter as such would not significantly affect the F-h curve. This includes modelling a rigid indenter as well as modelling both the indenter and the indenter holder.

3. Numerical Analysis

To characterize and compare a F-h curve to a target curve, the mean squared error (MSE) of the force in kN was used,

$$e^{(Y)} = \frac{1}{n}\sum_{i=1}^{n}(\hat{Y}_i - \hat{Y}_i)^2. \quad (2)$$

In usage, the quantity Y_i refers to the force at the specific location on the F-h curve, or $Y_i = f(h_i)$, where h_i is the displacement of the indenter. For the calculation of the MSE, 50 points on the loading portion of the F-h curve were used as the unloading portion of the curve would be governed by elastic deformation. To construct a surrogate model that allows efficient visualization of the data, a zero order radial basis surrogate model was used, given by Snyman and Wilke [5] as

$$f(\boldsymbol{x}) \approx \sum_{j=1}^{P} w_j \phi_j(\boldsymbol{x}, \boldsymbol{x}_c^j) = e^{(Y)}(\boldsymbol{x}). \quad (3)$$

The radial basis function, ϕ, used was the Gaussian function, which is computed using the distance between the model parameters, $\boldsymbol{x}$, to a series of preselected parameter values, $\boldsymbol{x}_c$, multiplied by some weighting, w, which will then equal the error function in Equation (2) at the preselected parameter values. The points used in the construction of the surrogate model were sampled uniformly from the parameter space. The parameters' values were normalized between ranges of -1 and 1 for the construction and use of the surrogate model.

4. Results

This section documents that valleys were found in the parameter space of the stress-strain model. Next it gives a brief overview of attempts to make the inverse problem well-posed, but the alternatives investigated failed to introduce sufficient information into the system to eliminate the presence of these valleys.

4.1. Parameter space

The parameter space for the saturation based material model given in (1) is $\boldsymbol{x} = \{b, m, \sigma_0\}$. In order to represent these parameter spaces, a target stress strain curve corresponding to b = 0.5, m = 5, and σ_0 = 350 MPa (Fig. 2) was selected. The radial basis function surrogate model given in Equation (3) of the MSE is then computed relative to this fixed curve. Fig. 3 (a), (b), and (c) show the contour plots of the MSE as a function of the parameter space when b, m and σ_0 are set at the target value respectively.

A deep valley (as opposed to a single distinct solution) is clearly present in each figure regardless of the parameter being held constant. The valleys aren't elongated ellipses, but rather distinct parabolic valleys. As such a line of potential solutions will be present, or something akin to a rotated set of axis in the full three-dimensional space for all three parameters.

The valleys result in a model which is significantly more insensitive in certain directions, that is directions parallel to the valleys. This would impact the performance of gradient based optimization techniques, as valleys result in difficulties found in many optimization test functions. An example test function would be Rosenbrock's banana function – which is known for poor algorithm performance due to its valley [6].

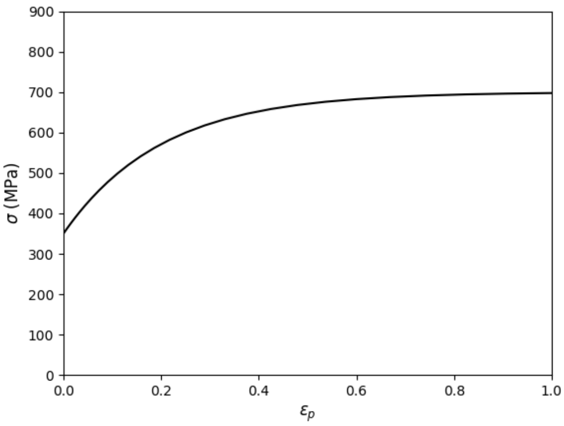

Fig. 2 Target stress-strain curve

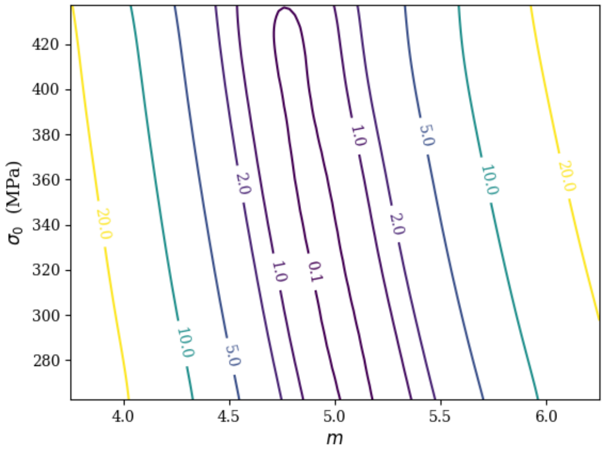

Fig. 3 (a) Contour plot of the MSE for the F-h curve with fixed b parameter

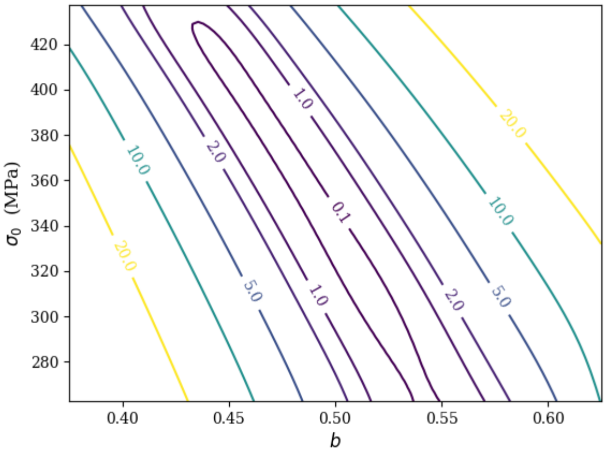

Fig. 3 (b) Contour plot of the MSE for the F-h curve with fixed m parameter

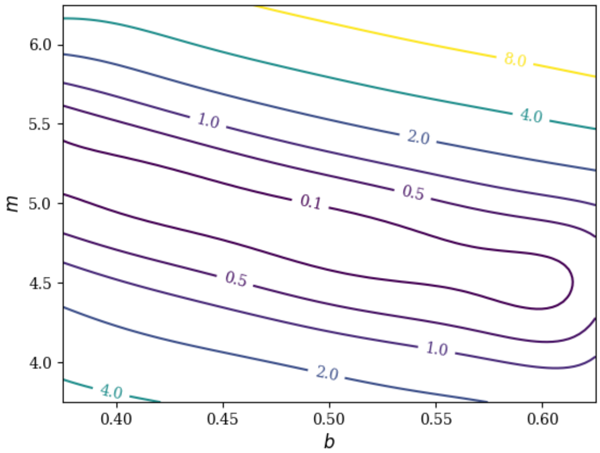

Fig. 3 (c) Contour plot of the MSE for the F-h curve with fixed σ_0 parameter

All the valleys show that certain parameters can vary by up to 50% without a drastic change in the error of the F-h curve. This shows that the virtual problem is ill-posed.

4.2. Differentiating between stress-strain curves

It is possible to find different parameter values for the stress strain model given in Equation (1) which will produce very similar F-h curves, as predicted by the valleys in Fig. 3. One such curve is presented here as the "worst fit" curve and is compared to the target curve used in the previous section. Fig. 4 shows the two stress-strain curves. Fig. 5 (a) also shows the corresponding F-h curves for the materials when loaded using multiple load displacements.

4.2.1. Inclusion of surface profile

One method for possibly distinguishing between the worst-fit description of the material and the true material is to include the unloaded surface profiles using different indentation depths. To facilitate this in a real experiment, several indentation tests can be done at different depths, and the surface profiles can be scanned. This was done numerically by running 3 different simulations that would have different final displacements. The three F-h curves and surface profiles for both the target and worst fit curves can be seen in Figures 5 (a) and 5 (b) respectively.

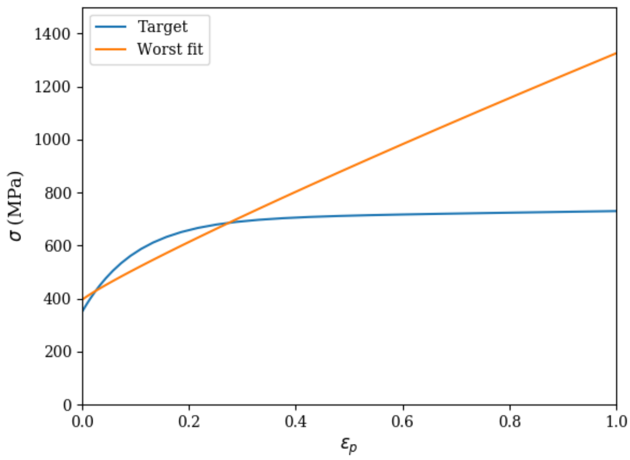

Fig. 4 Target and worst fit σ-ε_p curves

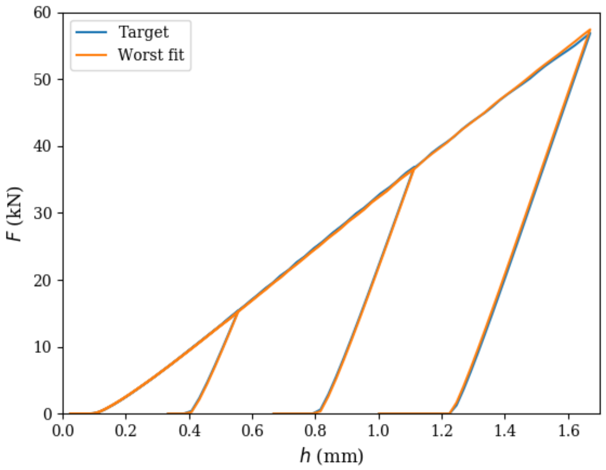

Fig. 5 (a) Target and worst fit F-h curves with multiple loading-unloading steps

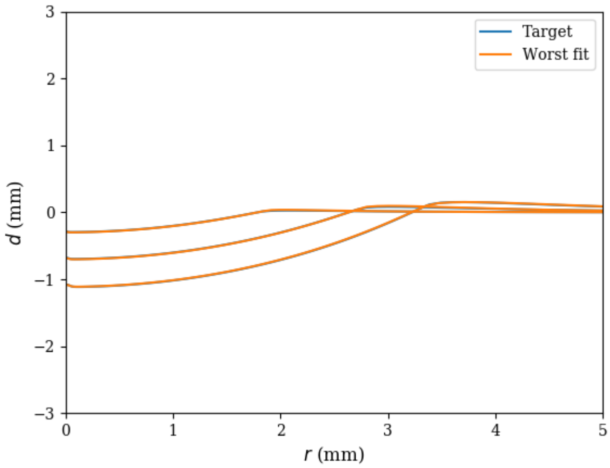

Fig. 5 (b) Target and worst fit surface profiles with multiple loading-unloading steps

Fig. 5 (b) shows that all the surface profiles are essentially superimposed, which shows that scanning the surface profile at various depths is not a feasible way to distinguish between the two materials.

4.2.2. Inclusion of a different indenter

Another possible method for recovering uniqueness would be to use a different indenter shape. Kang et al. [4, 7] suggested that multiple indenters should be used in order to bring uniqueness into the problem. However, Chen, et al. [7] brought up the issue of uniqueness in materials, even when using techniques commonly used to impose uniqueness to a problem such as multiple indenters. To investigate this, a non-rigid conical indenter was used. The conical indenter was also subjected to multiple loading-unloading steps as with the spherical indenter.

Figures 6 (a) and (b) show the conical indenter was also not able to sufficiently distinguish between the two curves with regards to the F-h curve or the surface profiles.

Chen et al. [7] found that with conical indenters at a variety of angles, it was still possible to find a family of solutions which would result in a many-to-one correspondence between σ-ε_p and F-h curves. Based on the observed results, it is also possible that a lack of uniqueness is present for families of indenter geometries, as two very different geometries were used.

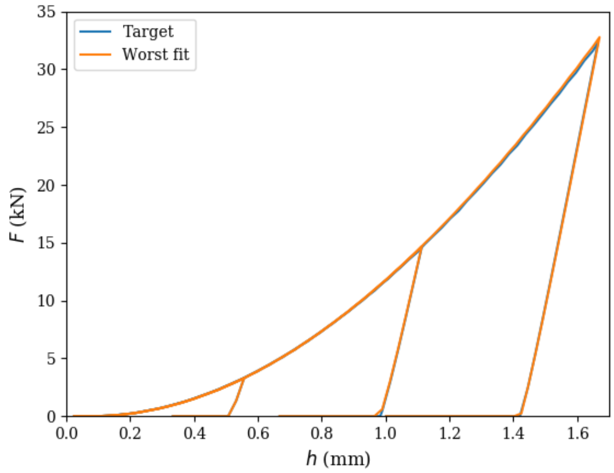

Fig. 6 (a) Target and worst fit F-h curves with multiple loading-unloading steps

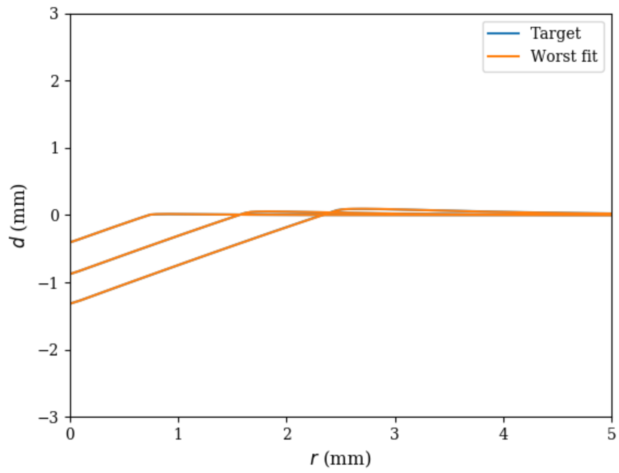

Fig. 6 (b) Target and worst fit surface profiles with multiple loading-unloading steps

5. Discussion

Many macroscopic observations of the indentation are not been able to distinguish between the two different σ-ε_p curves. For a possible explanation, consider the plastic-deformation work done by the indenter during indentation:

$$W^p = \int F dh\,. \tag{4}$$

The work is performed over the loading and unloading. The finite element model assumed to be an isotropic work hardening Von Mises material. Therefore the specific plastic-deformation work is given by Chakrabarty [8] as

$$dW_s^p = \hat{\sigma} d\hat{\varepsilon}_p. \tag{5}$$

The total plastic-deformation work performed during the indentation is given by

$$\begin{aligned} W^p &= \int W_s^p dV \\ &= \iint \hat{\sigma} d\hat{\varepsilon}_p dV\,. \end{aligned} \tag{6}$$

To be a match to the target F-h curve, the plastic deformation will have to perform the same amount of work as per Equation (4). It is conceivable that the stress and plastic strain distributions may vary in Equation (6), but in such a manner that the integral evaluates to the same value.

Figures 7 (a) and (b) show the stress distribution for the target and worst-fit material at an indentation depth of 1.4 mm, where Fig. 5 (a) shows that at this displacement the F-h curves are similar.

As can be seen in Fig. 7 (a), the maximum stress is indeed higher for the worst-fit model, which corresponds to the σ-ε_p curves in Fig. 4. This confirms that the two materials are in fact distinguishable materials.

Also shown in Fig. 7 (b) are the contours for the stresses of the target material, which encompass larger volumes than the worst-fit material's equivalent stress contours. This supports the idea that while higher stresses are present for the worst-fit material, these stresses are concentrated in smaller volumes. Therefore, when evaluating the integral in Equation (6), the average stress among these materials are identical.

However, the mechanisms which cause the stress distributions to act as such are unknown. One method of investigating these mechanisms would be to analyze the stress distributions directly under the indenter, giving insight into the stress distribution, and as such further work can be done on the topic.

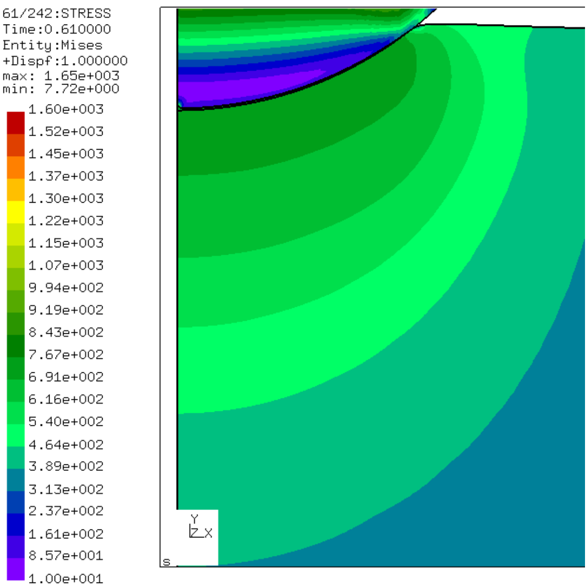

Fig. 7 (a) Stress distribution in target material

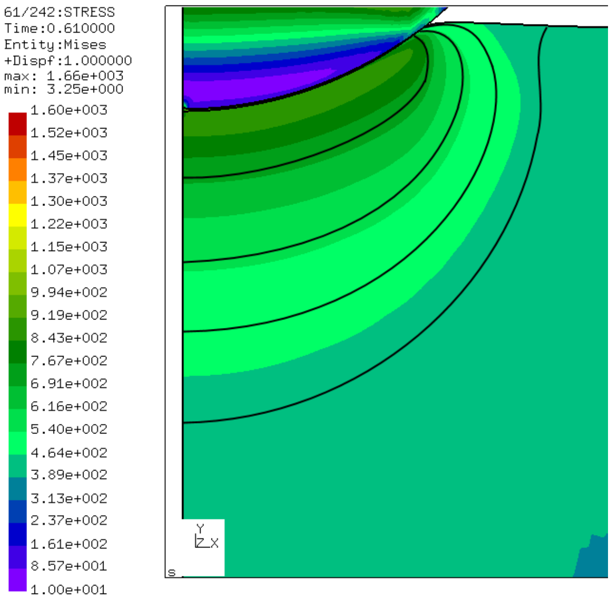

Fig. 7 (b) Stress distribution in worst-fit material with target material stress contours

6. Conclusion

It was possible to show that many different materials are able produce the same F-h curve during indentation. Furthermore, no practical techniques could be found which can distinguish between true and false solutions for the virtual problem. However, it was seen that the two solutions are in fact distinguishable if local measurements could be made rather than only measuring the total indenter reaction force.

However, as the results are contradictory to the current scientific community at large, the circumstances around the lack of uniqueness in the problem should be considered. It may be possible that the specific problem investigated may not be unique, but due to error in either the analysis or construction, it is not representative of the problem which the majority of authors have investigated. While the findings are not conclusive on the matter of general indentation tests, it certainly challenges the current assumption that the problem is generally well posed or that the uniqueness need not be investigated thoroughly.

References

[1] M. Beghini, L. Bertini and V. Fontanari, "Evaluation of the stress–strain curve of metallic materials," *International Journal of Solids and Structures,* vol. 43, pp. 2441-2459, 2006.

[2] E. Voce, "The relationship between stress and strain for homogeneous deformation," *Journal of the Institute of Metals,* vol. 74, pp. 537-562, 1948.

[3] T. Laursen and S. JC, "A study of the mechanics of microindentation using finite elements," *Journal of Materials Research,* vol. 7, no. 3, pp. 618-626, 1992.

[4] J. Kang, A. Becker and W. Sun, "A combined dimensional analysis and optimization approach for determining elastic-plastic properties from indentation tests," *Journal of Strain Analysis,* pp. 749-759, 2011.

[5] J. Snyman and D. Wilke, Practical Mathematical Optimisation, 2nd ed., Springer International Publishing, 2018.

[6] H. Rosenbrock, "An automatic method for finding the greatest or least value of a function," *The Computer Journal,* vol. 3, no. 3, pp. 175-184, 1960.

[7] X. Chen, N. Ogasawara, M. Zhao and N. Chiba, "On the uniqueness of measuring elastoplastic," *Journal of the Mechanics and Physics of Solids,* vol. 55, p. 1618–1660, 2007.

[8] J. Chakrabarty, Theory of Plasticity, 3rd ed., Burlington: Elsevier Butterworth-Heinemann, 2006.